C−H Bond Activation by Iridium(III) and Iridium(IV) Oxo Complexes

Tepaske, M.A.; Fitterer, A.; Verplancke, H.; Delony, D.; Neben, M.C.; de Bruin, B.; Holthausen, M.C.; Schneider, S.

DOI
10.1002/anie.202316729
10.1002/ange.202316729

Publication date
2024

Document Version
Final published version

Published in
Angewandte Chemie - International Edition

How to cite: *Angew. Chem. Int. Ed.* **2024**, *63*, e202316729
doi.org/10.1002/anie.202316729

C-H Activation

C–H Bond Activation by Iridium(III) and Iridium(IV) Oxo Complexes

Martijn A. Tepaske, Arnd Fitterer, Hendrik Verplancke, Daniel Delony, Marc C. Neben, Bas de Bruin, Max C. Holthausen, and Sven Schneider**

Abstract: Oxidation of an iridium(III) oxo precursor enabled the structural, spectroscopic, and quantum-chemical characterization of the first well-defined iridium(IV) oxo complex. Side-by-side examination of the proton-coupled electron transfer thermochemistry revealed similar driving forces for the isostructural oxo complexes in two redox states due to compensating contributions from H^+ and e^- transfer. However, C–H activation of dihydroanthracene revealed significant hydrogen tunneling for the distinctly more basic iridium-(III) oxo complex. Our findings complement the growing body of data that relate tunneling to ground state properties as predictors for the selectivity of C–H bond activation.

Metal oxo complexes are key species for biological and synthetic activation of strong C–H bonds via hydrogen atom abstraction (HAA).[1,2] Their examination also drove conceptual advances in proton-coupled electron transfer (PCET), as a physical basis to predict selectivities.[3,4] Bell–Evans–Polanyi-type (BEP) correlations of rates and substrate C–H bond dissociation (free) energies ($BD(F)E_{C-H}$) are common indicators for radical H-transfer. Within the Marcus framework for concerted PCET, BEP behavior can be attributed to linearization of the quadratic driving force dependence, assuming constant contributions from electron and proton tunneling.[5–7]

[*] M. A. Tepaske, Dr. D. Delony, M. C. Neben, Prof. Dr. S. Schneider
Georg-August-Universität, Institut für Anorganische Chemie
Tammanstraße 4, 37077 Göttingen (Germany)
E-mail: sven.schneider@chemie.uni-goettingen.de
A. Fitterer, H. Verplancke, Prof. Dr. M. C. Holthausen
Institut für Anorganische und Analytische Chemie, Goethe-Universität
Max-von-Laue-Straße 7, 60438 Frankfurt am Main (Germany)
E-mail: max.holthausen@chemie.uni-frankfurt.de
Prof. Dr. B. de Bruin
Homogeneous, Supramolecular and Bio-Inspired Catalysis Group, van't Hoff Institute for Molecular Sciences (HIMS)
Science Park 904, 1098XH Amsterdam (The Netherlands)

Recently, some oxo complexes showed significant deviations from BEP characteristics,[8] such as Anderson's Co^{III} (**A**) or Borovik's Mn^{IV} (**B**) complexes (Figure 1).[9,10] Due to their distinct basicity, unequal ("asynchronous") proton (PT) and electron transfer (ET) contributions to the PCET kinetics were proposed as origin.[11] Semiempirical parametrization was based on expansions of classical Marcus theory that weight the ET *vs.* PT driving forces[12] or add parameters that are defined by thermochemical descriptors of the reactants (E^0, pK_a).[13]

However, detailed C–H/D kinetic isotope effect (KIE) studies for **A** also indicated significant variation in H-tunneling contributions with different substrates.[14] Similar observations were reported for Tolman's distinctly basic copper(III) hydroxo complexes.[15] Shaik and co-workers ascribed deviations from BEP characteristics of a series of $Fe^{IV}O$ complexes to quantum-mechanical tunneling (QMT).[16] Intriguingly, more electron donating ligands increased QMT, which was attributed to narrower potential energy barriers that result from increased electrostatic interactions and smaller bonding asymmetry within the {MO···H···C} moiety.[17] Nevertheless, further systematic approaches are needed to develop reliable predictors for chemical reactivity under tunneling control.[18,19]

Substrate activation with oxo species in multiple redox states offers a potential strategy to systematically perturb their properties with minimal structural variation. Surprisingly, Borovik's oxo pair **B** and **C** (Figure 1) provides a unique example.[10,12] However, direct comparison of dihydroanthracene (DHA) activation was complicated by a mechanistic crossover from concerted PCET (**B**) to stepwise PT/ET (**C**).

We recently reported the formal iridium(III) oxo complex $[Ir^{III}(O)(PNP)]$ (**1**; PNP = N(CHCHP*t*Bu)$_2$).[20] Oxida-

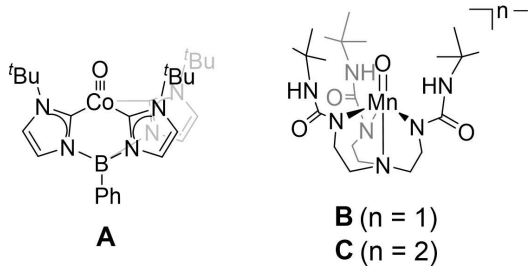

Figure 1. Examples for transition metal oxo complexes with "asynchronous" C–H abstraction characteristics.

tion of **1** now gave access to the first iridium(IV) oxo complex $[Ir^{IV}(O)(PNP)]^+$ ($\mathbf{1}^+$). Side-by-side isolation of **1** and $\mathbf{1}^+$ allowed for direct comparison of thermochemical and kinetic trends for C–H activation, revealing distinct differences in QMT that correlate with their relative basicity.

Complex **1** exhibits a triplet ground state with approximately even spin delocalization between the Ir and O atoms in the two orthogonal Ir–O π*-MOs, ($\rho_s(O) = 0.95$; $\rho_s(Ir) = 0.88$), resulting in net {•Ir=O•} oxyl character.[20] Electrochemical characterization revealed a reversible oxidation at $E^0 = -0.22$ V vs. $Fc^{+/0}$ (Figure S1).[21] Chemical oxidation of **1** in THF with $[FeCp_2]BAr^F{}_{24}$ ($BAr^F{}_{24}{}^- = B(C_6H_3\text{-}3,5\text{-}(CF_3)_2)_4{}^-$) results in rapid color change from purple to deep blue. UV/Vis titration at −30 °C (Figure 2a) displayed isosbestic points and constant product absorbance over several hours, indicating selective oxidation and sufficient chemical stability of $[Ir(O)(PNP)]^+$ ($\mathbf{1}^+$) for further characterization. $\mathbf{1}^+$ markedly decays at temperatures above 0 °C and conversion to mainly $[Ir(OH)(PNP)]^+$ ($\mathbf{2}^+$; 75 %)[20] is complete within 15 min at 20 °C (See ESI).

The formation of $\mathbf{1}^+$ was confirmed by X-ray crystallography (Figure 3),[22] allowing for structural comparison with parent **1**. Oxidation induces only little structural reorganization. Most prominently, the Ir–N distance significantly shortens ($\Delta d_{Ir-N} = -0.10$ Å) and the bond to the oxo ligand contracts slightly ($\Delta d_{Ir-O} = -0.02$ Å). These trends are in line with removal of an electron from a molecular orbital that has Ir–N and Ir–O antibonding character. In comparison, isoelectronic and isostructural $[Ir(N^tBu)(PNP)]^{0/+}$ exhibit more distinct oxidation-induced Ir=N^{t}Bu bond contraction ($\Delta d_{Ir-NtBu} = -0.06$ Å),[23] probably due to a higher degree of covalency.

Terminal oxo complexes of high-valent iridium were proposed as reactive intermediates in challenging transformations.[24–26] However, Wilkinson's closed-shell complex $[Ir^VO(Mes)_3]$ is the only well-defined example.[27] $\mathbf{1}^+$ exhibits a rhombic EPR spectrum (2-MeTHF, 29 K), which could be simulated for an S = 1/2 ground state (g = 1.98, 1.92, 1.58) with resolved ^{193}Ir and ^{31}P hyperfine interaction along g_1 (Figure 2b). The data exhibits significantly reduced g-anisotropy, as compared with the analogous nitrido and imido complexes $[Ir^{IV}N(PNP)]$ (g = 1.86, 1.58, 1.32) and $[Ir^{IV}(N^tBu)(PNP)]^+$ (g = 1.71, 1.63, 1.33).[23,28]

Accompanying DFT calculations at the SOC-ZORA–B3LYP/TZ2P–J level nicely reproduce the EPR data of $\mathbf{1}^+$ (g^{DFT} = 2.06, 1.92, 1.54) and support predominant π-oxyl character. The SOMO (Figure 2d) exhibits Ir–O π* antibonding character and is slightly polarized towards oxygen. Thus, oxidation of **1** depopulates one of the two π* SOMOs. Accordingly, the computed molecular structure of $\mathbf{1}^+$ reproduced the slight shortening of the Ir–O bond (Δd_{Ir-O}&ek; = −0.04 Å). The spin density (Figure 2e) is mainly distributed over the oxo ligand ($\rho_s(O) = 0.71$) and iridium ($\rho_s(Ir) = 0.44$) with significant spin polarization of the pincer ligand π system ($\rho_s(PNP) = -0.28$). Notably, oxidation significantly increases spin delocalization per e$^-$,

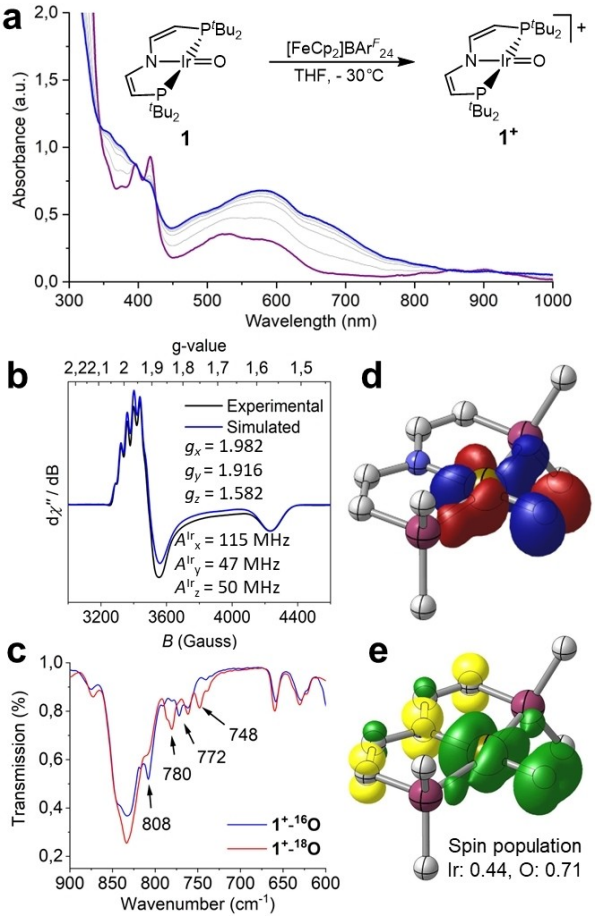

Figure 2. Spectroscopic and computational characterization of $\mathbf{1}^+$. **a**: UV/Vis titration of **1** with $[FeCp_2]BAr^F{}_{24}$ in THF. **b**: Experimental and simulated X-band EPR spectra of $\mathbf{1}^+$ in 2-MeTHF. **c**: IR spectra of $\mathbf{1}^+$ and $\mathbf{1}^+$-^{18}**O**. **d**/**e**: DFT computed SOMO (**d**) and spin-density (**e**) of $\mathbf{1}^+$ with Mulliken spin populations (isosurfaces at ±0.05 $a_0^{-3/2}$ and ±0.005 a_0^{-3}, respectively; methyl groups and H-atoms omitted for clarity).

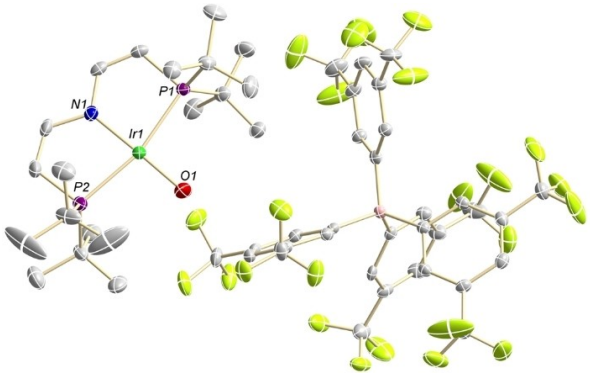

Figure 3. Molecular structure of $[\mathbf{1}^+]BAr^F{}_{24}$ from single-crystal X-ray diffraction with anisotropic displacement parameters at 50% probability. H-atoms, co-crystallized solvent and disorder are omitted for clarity. Selected bond lengths [Å] and angles [°]: Ir1–O1 1.803(4), Ir1–N1 1.939(3), N1–Ir1–O1 177.86(15).

leading to an inverted ligand field picture for $\{Ir–O\}^+$ π-bonding.[29]

This bonding picture is further supported by vibrational spectroscopy (Figure 2c). The Ir–O stretching mode of Wilkinson's $[IrO(Mes)_3]$ was assigned to a band at $\tilde{\nu}$ = 802 cm^{-1}.[27] In case of **1**$^+$, two bands at $\tilde{\nu}$ = 808 and 772 cm^{-1} were found in the Ir–O stretching region that shifted upon ^{18}O labelling ($\tilde{\nu}$ = 780 and 748 cm^{-1}). Anharmonic frequency calculations attribute this observation to the coupling of the Ir–O and the symmetric P–C stretching modes (see ESI). Mixing of M–O stretching vibrations with other modes was also reported for other oxo complexes.[30,31] Importantly, the experimental and computed data are significantly higher than the Ir–O stretching vibration found for **1** ($\tilde{\nu}$ = 743 cm^{-1}, $\Delta\tilde{\nu}_{BP86}$ = 53 cm^{-1}), which is in line with electron removal from an MO with π^*_{Ir-O} character.

With the isostructural oxo redox couple at hand, the impact on the PCET thermochemistry was examined in THF. The square scheme (Scheme 1) was experimentally anchored with the iridium(III/II) hydroxo and iridium(IV/III) oxo redox potentials, as well as the O–H bond dissociation free energy ($BDFE_{O-H}$) of **2** obtained by titration calorimetry.[32] All other values were calculated with Bordwell's equation,

$$BDFE = 23.06 \cdot E^0 + 1.37 \cdot pK_a + C_G \quad (1)$$

using Mayer's standard potential for the H^+/H couple in THF *vs.* Fc^+/Fc (C_G = 59.9 kcal mol^{-1}).[33]

Notably, the two PCET couples, **2**/**1** and **2**$^+$/**1**$^+$, exhibit only slightly different O–H bond strengths ($\Delta BDFE_{O-H}$ = 3 kcal mol^{-1}). ONIOM(CC:DFT) computations are in excellent agreement with experiment ($BDFE^{ONIOM}_{O-H}$(**2**) = 73.6 kcal mol^{-1}, $BDFE^{ONIOM}_{O-H}$(**2**$^+$) = 74.8 kcal mol^{-1}). The small difference coincides with slightly different spin-orbit contributions, which are larger for the iridium(IV/III) PCET couple ($\Delta\Delta E^{SOC}_{O-H}$ = 1.5 kcal mol^{-1}, see ESI). We note, however, that the differential spin-orbit effect is of the same magnitude as experimental error. The experimental data also offers the O–H hydricity of **2** ($\Delta G^0_{H^-}$ = 94 ± 2 kcal mol^{-1}; see ESI).[34]

The close O–H bond strengths of **2** and **2**$^+$ reveal almost fully compensating contributions from PT and ET driving forces. **1** exhibits relatively high basicity (pK_a(**2**$^+$) = 17), which is close to Tolman's copper hydroxide complexes.[15] While the basicity of **1**$^+$ was not directly obtained, the $BDFE_{O-H}$ of **2**$^+$ and the absence of an oxidation within the accessible potential window ($E > +1.5$ V) suggest a pK_a below 0 for hypothetical $[Ir^{IV}(OH)(PNP)]^{2+}$, i.e., over 17 pK_a units lower than that of **2**$^+$. Interestingly, Borovik's oxo redox pair **B**/**C** (Figure 1) exhibits a much larger difference in PCET driving force ($\Delta BDFE_{O-H}$ = 12 kcal mol^{-1}). While the origin of this observation is not known, it is tempting to speculate that the amide substituents, which frame the bonding pocket, dampen the PT driving force of the oxidized Mn^{IV} hydroxo complex due to adaptive hydrogen bonding.

The almost identical $BDFE_{O-H}$ of **1** and **1**$^+$ provide an ideal case to compare HAA with reference substrate DHA ($BDFE_{C-H}{}^{THF}$ = 73.8 kcal mol^{-1}). In both cases, anthracene was formed selectively, accompanied by the hydroxo complexes **2** and **2**$^+$, respectively. UV/Vis kinetics under pseudo-first-order conditions showed clean isosbestic points (Figure S9). The second-order rate constant obtained for **1** (k_2 = 0.013 ± 0.005 M^{-1} s^{-1}, Table 1) is around an order of magnitude smaller than that of **1**$^+$ (k_2 = 0.29 ± 0.03 M^{-1} s^{-1}), which is in line with the slightly lower PCET driving force.

Potential PCET mechanisms were evaluated by comparison of the kinetic and thermochemical data. The low reduction potential and negligible basicity of **1**$^+$ safely exclude stepwise ET/PT paths for both and PT/ET for **1**$^+$. For **1**, the relative acidities of **2**$^+$ and DHA ($\Delta pK_a{}^{THF} \approx 26$; see ESI),[35] locate the PT products **2**$^+$/$C_{14}H_9^-$ at $\Delta G^0 \approx$ +35 kcal mol^{-1} above parent **1**/DHA, which is well beyond the effective reaction barrier (Table 1). Thus, PT/ET as reported for **C**, can also be dismissed for **1**. The high hydricity of **2** ($\Delta G^0_{H^-}$ > 94 ± 2 kcal mol^{-1}) leaves initial hydride transfer as potential route for **1**$^+$ and was computed to be only slightly endergonic ($\Delta G^{0,ONIOM}$ = 2.0 kcal mol^{-1}). H^- transfer was initially proposed for benzylic C–H

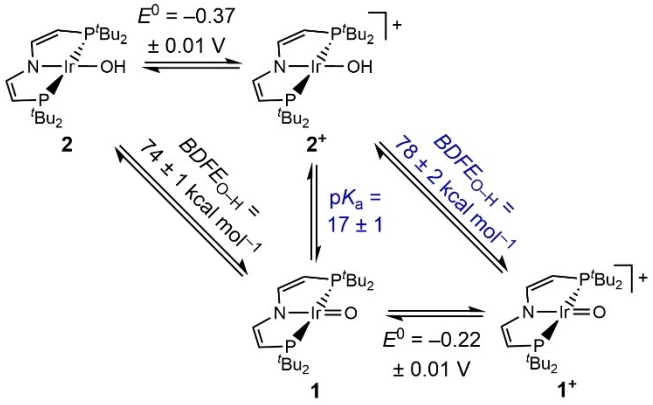

Scheme 1. Thermochemical square scheme for PCET in THF; experimental data in black and blue values were calculated via Bordwell's equation (eq. 1).

Table 1: Kinetic data for HAA from dihydroanthracene with **1**, **1**$^+$, **B** and **C** (n.a. = not available).

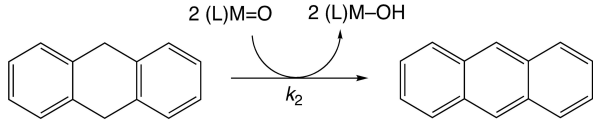

(L)M=O	**1**	**1**$^+$	**C** [10]	**B** [10]
solvent	*THF*		*DMSO*	
k_2 ($M^{-1}s^{-1}$)[c]	0.013 ± 0.005	0.29 ± 0.03	0.48(4)	0.026(2)
$\Delta H^{\ddagger}$ [a]	9.3 ± 0.3	8.1 ± 0.9	14(2)	5(1)
$\Delta S^{\ddagger}$ [b]	−35 ± 1	−35 ± 4	−14(6)	−49(4)
$\Delta G^{\ddagger}$ [a,c]	20 ± 1	18 ± 4	18(3)	19(2)
k_H/k_D	24 ± 7	8 ± 3	2.6	6.8
$\Delta E_a{}^{D-H}$ [a]	3.7 ± 0.6	2 ± 1	n.a.	n.a.
$\ln(A_H/A_D)$	−3.2 ± 0.9	−1 ± 2	n.a.	n.a.

[a] in kcal mol^{-1}. [b] in cal mol^{-1} K^{-1}. [c] at 293 K.

activation with Ru^{IV} oxo complexes,[36] but later dismissed.[37] Eyring analysis gave identical activation entropies for both **1** and $\mathbf{1}^+$ (Table 1),[38] suggesting closely related transition states and solvent reorganization. This, however, seems unlikely for mechanisms with significantly different degrees of charge separation. For example, Borovik's oxo complexes exhibit significantly different $\Delta S^{\ddagger}$ for concerted PCET (**B**) vs. PT/ET (**C**) mechanisms (Table 1). Furthermore, quantum-chemical analysis supports radical pathways rather than hydride transfer for both **1** and $\mathbf{1}^+$ (see section 3.7 of the ESI).

Thus, our data support concerted PCET (or hydrogen atom transfer, HAT) for both oxo complexes. However, the kinetic isotope effects ($KIE = k_H/k_D$) with DHA-d_4, revealed distinct differences regarding contributions from QMT. The high KIE_{293K} of **1** (Table 1) suggests significant tunneling, while that of $\mathbf{1}^+$ is close to the semi-classical limit, which arises from zero-point energy (ZPE) differences of the high energy stretching modes. This was confirmed by Arrhenius analysis of the temperature dependence (Figure 4) to separate semi-classical (ΔE_a) from QMT contributions expressed by the pre-exponential factors (A):[39]

$$ln\frac{k_H}{k_D} = ln\frac{A_H}{A_D} + \frac{E_a(D) - E_a(H)}{RT} \quad (2)$$

The Arrhenius parameters of $\mathbf{1}^+$ confirmed minor QMT contributions. ΔE_a (2 ± 1 kcal mol^{-1} = 700 ± 350 cm^{-1}) is close to $\Delta ZPE_{\nu(C\text{–}H/D)}$ and should be higher for pronounced thermally activated tunneling. Furthermore, the ratio of the pre-exponential factors is close to unity ($\ln(A_H/A_D) = -1 \pm 2$), as expected within Bell's semi-classical KIE model.[40,41] In contrast, the much steeper Arrhenius slope ($\Delta E_a = 3.7 \pm 0.6$) kcal mol^{-1}) and largely differing pre-exponential factors ($\ln(A_H/A_D) = -3.2 \pm 0.9$) of **1** are well outside the semi-classical framework, indicating significant QMT contributions. Notably, almost identical Arrhenius parameters were obtained for complex **A**.

Quantum chemical assessment based on ONIOM(CC:DFT) computations gave activation barriers of $\Delta G^{\ddagger} =$ 19.5 kcal mol^{-1} (**TS1**) and 21.0 kcal mol^{-1} ($\mathbf{TS1}^+$). Both barriers include atom tunneling contributions (**TS1**: -2.4 kcal mol^{-1}, $\mathbf{TS1}^+$: -1.0 kcal mol^{-1}), which were obtained based on an Eckart potential[42] as implemented in the POLYRATE program.[43] Fitted to the ZPVE-corrected relative energies of reactants, transition states and products, the Eckart model gave H/D KIEs within experimental error (**1**: 29, $\mathbf{1}^+$: 11). The larger QMT contribution for **1** is attributed to a narrower potential, characterized by a larger imaginary vibrational frequency of the transition state (**TS1**: i2139 cm^{-1}, $\mathbf{TS1}^+$: i1520 cm^{-1}; Figure 4). Adopting Shaik's approach for KIE analysis,[17] barrier narrowness can be linked to the electrostatic potentials within the $\{IrO\cdots H\cdots C\}^{0/+}$ moieties: **TS1** exhibits a markedly more negative partial charge of the oxygen atom and a higher O–H bond order compared to $\mathbf{TS1}^+$ (Figure 4). We thus attribute the larger H-atom tunneling contribution to the KIE with **1** to its distinctly higher basicity.

In summary, oxidation of **1** enabled the isolation of the first terminal iridium(IV) oxo complex. Spectroscopic, structural, and quantum-chemical data confirmed the electronic structure picture that was reported for the triplet precursor: Removal of an unpaired electron from a π* MO strengthens the Ir–O bond of $\mathbf{1}^+$ and generates a doublet ground state with predominant oxyl character. Notably, oxidation hardly affects the $1e^-/1H^+$ PCET thermochemistry due to almost fully compensating PT and ET contributions. In consequence, the experimental and computational data for C–H activation of DHA support concerted radical mechanisms in both cases with similar rates and activation parameters. However, KIE analysis revealed significant acceleration for **1** due to H-tunneling. Following Shaik's approach, we attribute this observation to its higher basicity ($\Delta pK_a > 17$), resulting in a narrower barrier with increased QMT probability. Importantly, our results complement those of Anderson for a basic cobalt(III) oxo complex (**A**) with significant deviations from BEP behavior,[9,14] but also those for Tolman's distinctly basic copper(III) hydroxo complexes.[15] The growing number of examples thus suggests that thermochemical data might be useful predictors for C–H activation selectivities under QMT control.

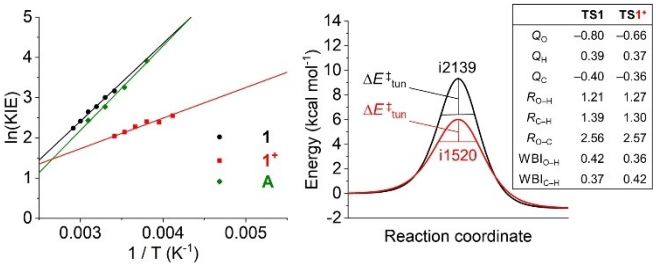

Figure 4. Experimental and quantum-chemical examination of QMT for **1** (black) and $\mathbf{1}^+$ (red). *Left*: Arrhenius plots of the C–H/D KIE with DHA vs. DHA-d_4 and comparison Anderson's cobalt(III) oxo complex **A** (green).[14] *Right*: Eckart potentials based on ZPVE-corrected relative energies of reactants, transition states, and products for DHA with selected atomic NPA charges (Q), interatomic distances (R in Å), and Wiberg bond indices (WBI) at the transition state structures as used for Shaik's KIE analysis.

Supporting Information

The authors have cited additional references within the Supporting Information.[44–107]

Acknowledgements

This work was funded by the Deutsche Forschungsgemeinschaft (DFG, 389479699/RTG2455). Dr. A.C. Stückl is acknowledged for measuring EPR spectra and Dr. M. Otte for crystallographic data acquisition. Quantum chemical calculations of the Frankfurt group were performed at the Center for Scientific Computing (CSC) Frankfurt on the Goethe-HLR computer cluster. We thank Dr. Urs Gellrich and Jama Ariai (Univ. Giessen) for providing their entropy

correction code. Open Access funding enabled and organized by Projekt DEAL.

Conflict of Interest

The authors declare no conflict of interest.

Data Availability Statement

The data that support the findings of this study are available from the corresponding author upon reasonable request.

Keywords: C–H Activation · Oxo Complexes · Quantum Chemistry · Tunneling

[1] A. Gunay, K. H. Theopold, *Chem. Rev.* **2010**, *110*, 1060.
[2] A. R. McDonald, L. Que, *Coord. Chem. Rev.* **2013**, *257*, 414.
[3] J. M. Mayer, *Acc. Chem. Res.* **2011**, *44*, 36.
[4] X. S. Xue, P. Ji, B. Zhou, J. P. Cheng, *Chem. Rev.* **2017**, *117*, 8622.
[5] J. W. Darcy, B. Koronkewicz, G. A. Parada, J. M. Mayer, *Acc. Chem. Res.* **2018**, *51*, 2391.
[6] R. Tyburski, T. Liu, S. D. Glover, L. Hammarström, *J. Am. Chem. Soc.* **2021**, *143*, 560.
[7] S. Hammes-Schiffer, *J. Am. Chem. Soc.* **2015**, *137*, 8860.
[8] D. Usharani, D. C. Lacy, A. S. Borovik, S. Shaik, *J. Am. Chem. Soc.* **2013**, *135*, 17090.
[9] M. K. Goetz, J. S. Anderson, *J. Am. Chem. Soc.* **2019**, *141*, 4051.
[10] T. H. Parsell, M. Y. Yang, A. S. Borovik, *J. Am. Chem. Soc.* **2009**, *131*, 2762.
[11] D. Bím, M. Maldonado-Domínguez, L. Rulísek, M. Srnec, *Proc. Natl. Acad. Sci. USA* **2018**, *115*, E10287.
[12] S. K. Barman, M. Y. Yang, T. H. Parsell, M. T. Green, A. S. Borovik, *Proc. Natl. Acad. Sci. USA* **2021**, *118*, e2108648118.
[13] M. Maldonaldo-Domínguez, M. Srnec, *Inorg. Chem.* **2022**, *61*, 18811.
[14] J. E. Schneider, M. K. Goetz, J. S. Anderson, *Chem. Commun.* **2023**, *59*, 8584.
[15] D. Dhar, G. M. Yee, A. D. Spaeth, D. W. Boyce, H. Zhang, B. Dereli, C. J. Cramer, W. B. Tolman, *J. Am. Chem. Soc.* **2016**, *138*, 356.
[16] D. Mandal, R. Ramanan, D. Usharani, D. Janardanan, B. Wang, S. Shaik, *J. Am. Chem. Soc.* **2015**, *137*, 722.
[17] D. Mandal, D. Mallick, S. Shaik, *Acc. Chem. Res.* **2018**, *51*, 107.
[18] P. R. Schreiner, *Trends Chem.* **2020**, *2*, 980.
[19] T. Constantin, B. Górski, M. J. Tilby, S. Chelli, F. Juliá, J. Llaveria, K. J. Gillen, H. Zipse, S. Lakhdar, D. Leonori, *Science* **2022**, *377*, 1323.
[20] D. Delony, M. Kinauer, M. Diefenbach, S. Demeshko, C. Würtele, M. C. Holthausen, S. Schneider, *Angew. Chem. Int. Ed.* **2019**, *58*, 10971.
[21] Improved referencing led to slight correction of the initially reported potential in ref. [20].
[22] Deposition number 2305524 contains the supplementary crystallographic data for this paper. These data are provided free of charge by the joint Cambridge Crystallographic Data Centre and Fachinformationszentrum Karlsruhe Access Structures service.
[23] M. Kinauer, M. Diefenbach, H. Bamberger, S. Demeshko, E. J. Reijerse, C. Volkmann, C. Würtele, J. Van Slageren, B. De Bruin, M. C. Holthausen, S. Schneider, *Chem. Sci.* **2018**, *9*, 4325.
[24] a) J. F. Hull, D. Balcells, J. D. Blakemore, C. D. Incarvito, O. Eisenstein, G. W. Brudvig, R. H. Crabtree, *J. Am. Chem. Soc.* **2009**, *131*, 8730; b) L. S. Sharninghausen, S. B. Sinha, D. Y. Shopov, B. Choi, B. Q. Mercado, X. Roy, D. Balcells, G. W. Brudvig, R. H. Crabtree, *J. Am. Chem. Soc.* **2016**, *138*, 15917.
[25] a) M. Zhou, N. D. Schley, R. H. Crabtree, *J. Am. Chem. Soc.* **2010**, *132*, 12550; b) M. Zhou, D. Balcells, A. R. Parent, R. H. Crabtree, O. Einstein, Eisenstein, *ACS Catal.* **2012**, *2*, 208.
[26] S. Fukuzumi, T. Kobayashi, T. Suenobu, *J. Am. Chem. Soc.* **2010**, *132*, 11866.
[27] R. S. Hay-Motherwell, G. Wilkinson, B. Hussain-Bates, M. B. Hursthouse, *Polyhedron* **1993**, *12*, 2009.
[28] M. G. Scheibel, B. Askevold, F. W. Heinemann, E. J. Reijerse, B. de Bruin, S. Schneider, *Nat. Chem.* **2012**, *4*, 552.
[29] R. Hoffmann, S. Alvarez, C. Mealli, A. Falceto, T. J. Cahill III, T. Zeng, G. Manca, *Chem. Rev.* **2016**, *116*, 8173.
[30] E. Andris, R. Navrátil, J. Jašík, M. Srnec, M. Rodríguez, M. Costas, J. Roithová, *Angew. Chem. Int. Ed.* **2019**, *58*, 9619.
[31] J. England, J. Prakash, M. A. Cranswick, D. Mandal, Y. Guo, E. Münck, S. Shaik, L. Que, *Inorg. Chem.* **2015**, *54*, 7828.
[32] The previously reported $BDFE_{O–H}$ of **2** (ref. [20]) was corrected by using the recently updated $BDFE_{O–H}$ of the PCET reference compound (2,4,6-tritertbutylphenoxyl) and the free energy of the hydrogen atom in THF (C_G); see ESI for further information.
[33] R. G. Agarwal, S. C. Coste, B. D. Groff, A. M. Heuer, H. Noh, G. A. Parada, C. F. Wise, E. M. Nichols, J. J. Warren, J. M. Mayer, *Chem. Rev.* **2022**, *122*, 1.
[34] K. R. Brereton, C. N. Jadrich, B. M. Stratakes, A. J. M. Miller, *Organometallics* **2019**, *38*, 3104.
[35] F. G. Bordwell, *Pure Appl. Chem.* **1977**, *49*, 963.
[36] M. S. Thompson, T. J. Meyer, *J. Am. Chem. Soc.* **1982**, *104*, 5070.
[37] J. R. Bryant, J. M. Mayer, *J. Am. Chem. Soc.* **2003**, *125*, 10351.
[38] Note that conventional Eyring analysis neglects contributions from quantum-chemical tunneling (QMT), which can offset $\Delta S^{\ddagger}$.
[39] J. P. Klinman, A. R. Offenbacher, *Acc. Chem. Res.* **2018**, *51*, 1966.
[40] R. P. Bell, *The Tunnel Effect in Chemistry*, Springer, New York, **1980**, p. 106.
[41] M. E. Schneider, M. J. Stern, *J. Am. Chem. Soc.* **1972**, *94*, 1517.
[42] a) C. Eckart, *Phys. Rev.* **1930**, *35*, 1303; b) A. Gonzalez-Lafont, T. N. Truong, D. G. Truhlar, *J. Chem. Phys.* **1991**, *95*, 8875.
[43] J. Zheng, J. L. Bao, R. Meana-Pañeda, S. Zhang, B. J. Lynch, J. C. Corchado, Y.-Y. Chuang, P. L. Fast, W.-P. Hu, Y.-P. Liu, G. Lynch, K. A. Nguyen, C. F. Jackels, A. Fernandez Ramos, B. A. Ellingson, V. S. Melissas, J. Villà, I. Rossi, E. L. Coitiño, J. Pu, T. V. Albu, A. Ratkiewicz, R. Steckler, B. C. Garrett, A. D. Isaacson, D. G. Truhlar, *Polyrate*-version 2017-C, University of Minnesota, Minneapolis (USA), **2017**.
[44] C. R. Goldsmith, R. T. Jonas, T. D. P. Stack, *J. Am. Chem. Soc.* **2002**, *124*, 83.
[45] J. Le Bras, H. Jiao, W. E. Meyer, F. Hampel, J. A. Gladysz, *J. Organomet. Chem.* **2000**, *616*, 54.
[46] J. Meiners, A. Friedrich, E. S. Herdtweck, S. Schneider, *Organometallics* **2009**, *28*, 6331.
[47] A. L. Onderdelinden, A. van der Ent, *Inorg. Chim. Acta* **1972**, *6*, 420.
[48] J. Meiners, M. G. Scheibel, M. H. Lemée-Cailleau, S. A. Mason, M. B. Boeddinghaus, T. F. Fässler, E. Herdtweck,

M. M. Khusniyarov, S. Schneider, *Angew. Chem. Int. Ed.* **2011**, *50*, 8184.
[49] C. Garland, J. Nibler, D. Shoemaker, *Experiments in Physical Chemistry*, McGraw-Hill, New York, **2009**, p. 38.
[50] M. H. Abraham, P. L. Grellier, D. V. Prior, P. P. Duce, J. J. Morris, P. J. Taylor, *J. Chem. Soc. Perkin Trans. 2* **1989**, *0*, 699.
[51] M. H. Abraham, P. L. Grellier, D. V. Prior, J. J. Morris, P. J. Taylor, *J. Chem. Soc. Perkin Trans. 2* **1990**, 521.
[52] J. J. Warren, T. A. Tronic, J. M. Mayer, *Chem. Rev.* **2010**, *110*, 6961.
[53] E. Brunner, *J. Chem. Eng. Data* **1985**, *30*, 269.
[54] "Hydrogen and Deuterium": C. Young, *Solubility Data Series*, *Vol. 5*, Pergamon Press, New York, **1981**, p. 646.
[55] F. Ding, J. M. Smith, H. Wang, *J. Org. Chem.* **2009**, *74*, 2679.
[56] K. Abdur-Rashid, T. P. Fong, B. Greaves, D. G. Gusev, J. G. Hinman, S. E. Landau, A. J. Lough, R. H. Morris, *J. Am. Chem. Soc.* **2000**, *122*, 9155.
[57] X. Zhang, F. G. Bordwell, *J. Org. Chem.* **1992**, *57*, 4163.
[58] a) APEX3 v2016.9–0 (SAINT/SADABS/SHELXT/SHELXL), Bruker AXS Inc., Madison (USA), **2016**; b) G. M. Sheldrick, *Acta Crystallogr. Sect. A* **2015**, *71*, 3; c) G. M. Sheldrick, *Acta Crystallogr. Sect. C* **2015**, *71*, 3; d) G. M. Sheldrick, *Acta Crystallogr. Sect. A* **2008**, *64*, 112.
[59] a) "Software update: the ORCA program system, version 4.0": F. Neese, *Wiley Interdiscip. Rev.: Comput. Mol. Sci.* **2012**, *2*, 73; b) "Software Update: The ORCA Program System Version 5.0": F. Neese, *Wiley Interdiscip. Rev.: Comput. Mol. Sci.* **2022**, *12*, e1606.
[60] P. J. Stephens, F. J. Devlin, C. F. Chabalowski, M. J. Frisch, *J. Phys. Chem.* **1994**, *98*, 11623.
[61] F. Weigend, R. Ahlrichs, *Phys. Chem. Chem. Phys.* **2005**, *7*, 3297.
[62] D. Andrae, U. Häußermann, M. Dolg, H. Stoll, H. Preuß, *Theor. Chim. Acta* **1990**, *77*, 123.
[63] S. Grimme, S. Antony, S. Ehrlich, H. Krieg, *J. Chem. Phys.* **2010**, *132*, 154104.
[64] A. V. Marenich, C. J. Cramer, D. G. Truhlar, *J. Phys. Chem. B* **2009**, *113*, 6378.
[65] J. Ariai, U. Gellrich, *Phys. Chem. Chem. Phys.* **2023**, *25*, 14005.
[66] A. J. Garza, *J. Chem. Theory Comput.* **2019**, *15*, 3204.
[67] E. D. Glendening, J. K. Badenhoop, A. E. Reed, J. E. Carpenter, J. A. Bohmann, C. M. Morales, C. R. Landis, F. Weinhold, NBO 6.0. University of Wisconsin, Madison (USA), **2013**.
[68] A. D. Becke, *Phys. Rev. A* **1988**, *38*, 3098.
[69] J. P. Perdew, W. Yue, *Phys. Rev. B* **1986**, *33*, 8800.
[70] M. J. Frisch, G. W. Trucks, H. B. Schlegel, G. E. Scuseria, M. A. Robb, J. R. Cheeseman, G. Scalmani, V. Barone, G. A. Petersson, H. Nakatsuji, X. Li, M. Caricato, A. V. Marenich, J. Bloino, B. G. Janesko, R. Gomperts, B. Mennucci, H. P. Hratchian, J. V. and others. Gaussian 16, Revision B.01. Gaussian Inc., Wallingford (USA), **2016**.
[71] M. Svensson, S. Humbel, R. D. J. Froese, T. Matsubara, S. Sieber, K. Morokuma, *J. Phys. Chem.* **1996**, *100*, 19357.
[72] M. Svensson, S. Humbel, K. Morokuma, *J. Chem. Phys.* **1996**, *105*, 3654.
[73] T. B. Adler, G. Knizia, H. J. Werner, *J. Chem. Phys.* **2007**, *127*, 221106.
[74] H. J. Werner, P. J. Knowles, G. Knizia, G, F. R. Manby, M. Schütz, P. Celani, W Györffy, D. Kats, T. Korona, R. Lindh and others. MOLPRO, Version 2020, a Package of Ab Initio Programs, University College Cardiff Consultants Ltd., Cardiff (UK), **2020**.
[75] G. Knizia, T. B. Adler, H. J. Werner, *J. Chem. Phys.* **2009**, *130*, 54104.
[76] K. A. Peterson, T. B. Adler, H. J. Werner, *J. Chem. Phys.* **2008**, *128*, 84102.
[77] D. Figgen, K. A. Peterson, M. Dolg, H. Stoll, *J. Chem. Phys.* **2009**, *130*, 164108.
[78] K. E. Yousaf, K. A. Peterson, *J. Chem. Phys.* **2008**, *129*, 184108.
[79] S. Kritikou, J. G. Hill, *J. Chem. Theory Comput.* **2015**, *11*, 5269.
[80] F. Weigend, *J. Comput. Chem.* **2008**, *29*, 167.
[81] J. G. Hill, *J. Chem. Phys.* **2011**, *135*, 44105.
[82] C. Riplinger, P. Pinski, U. Becker, E. F. Valeev, F. Neese, *J. Chem. Phys.* **2016**, *144*, 024109.
[83] T. H. Dunning, *J. Chem. Phys.* **1989**, *90*, 1007.
[84] R. A. Kendall, T. H. Dunning, R. J. Harrison, *J. Chem. Phys.* **1992**, *96*, 6796.
[85] D. E. Woon, T. H. Dunning, *J. Chem. Phys.* **1993**, *98*, 1358.
[86] F. Weigend, A. Köhn, C. Hättig, A. Kö, F. Karlsruhe, *J. Chem. Phys.* **2002**, *116*, 3175.
[87] C. Angeli, R. Cimiraglia, S. Evangelisti, T. Leininger, J. P. Malrieu, *J. Chem. Phys.* **2001**, *114*, 10252.
[88] C. Angeli, R. Cimiraglia, J. P. Malrieu, *Chem. Phys. Lett.* **2001**, *350*, 297.
[89] C. Angeli, R. Cimiraglia, J. P. Malrieu, *J. Chem. Phys.* **2002**, *117*, 9138.
[90] B. A. Heß, C. M. Marian, U. Wahlgren, O. Gropen, *Chem. Phys. Lett.* **1996**, *251*, 365.
[91] E. van Lenthe, E. J. Baerends, J. G. Snijders, *J. Chem. Phys.* **1993**, *99*, 4597.
[92] E. van Lenthe, E. J. Baerends, J. G. Snijders, *J. Chem. Phys.* **1994**, *101*, 9783.
[93] E. van Lenthe, J. G. Snijders, E. J. Baerends, *J. Chem. Phys.* **1996**, *105*, 6505.
[94] C. van Wüllen, *J. Chem. Phys.* **1998**, *109*, 392.
[95] D. A. Pantazis, X, Y. Chen, C. R. Landis, F. Neese, *J. Chem. Theory Comput.* **2008**, *4*, 908.
[96] G. L. Stoychev, A. A. Auer, F. Neese, *J. Chem. Theory Comput.* **2017**, *13*, 554.
[97] G. te Velde, F. M. Bickelhaupt, E. J. Baerends, C. Fonseca Guerra, S. J. A. van Gisbergen, J. G. Snijders, T. Ziegler, *J. Comput. Chem.* **2001**, *22*, 931.
[98] E. Van Lenthe, E. J. Baerends, *J. Comput. Chem.* **2003**, *24*, 1142.
[99] S. K. Wolff, T. Ziegler, E. van Lenthe, E. J. Baerends, *J. Chem. Phys.* **1999**, *110*, 7689.
[100] B. C. Garrett, D. G. Truhlar, R. S. Grev, A. W. Magnuson, *J. Chem. Phys.* **1980**, *84*, 1730.
[101] A. Kuppermann, D. G. Truhlar, *J. Am. Chem. Soc.* **1971**, *93*, 1840.
[102] D. G. Truhlar, A. D. Isaacson, B. C. Garrett, *Theory of Chemical Reaction Dynamics*, CRC Press, Boca Raton, **1985**, p. 65.
[103] D. Mallick, S. Shaik, *J. Am. Chem. Soc.* **2017**, *139*, 11451.
[104] S. Ilic, A. Alherz, C. B. Musgrave, K. D. Glusac, *Chem. Soc. Rev.* **2018**, *47*, 2809.
[105] J. Cheng, K. L. Handoo, V. D. Parker, *J. Am. Chem. Soc.* **1993**, *115*, 2655.
[106] D. Mallick, S. Shaik, *J. Am. Chem. Soc.* **2017**, *139*, 11451.
[107] J. E. M. N. Klein, D. Mandal, W.-M. Ching, D. Mallick, L. Que Jr., S. Shaik, *J. Am. Chem. Soc.* **2017**, *139*, 18705.

Manuscript received: November 3, 2023
Accepted manuscript online: December 20, 2023
Version of record online: January 10, 2024